Rotaxanes

DOI: 10.1002/ange.200501761

Complexation-Induced Translational Isomerism: Shuttling through Stepwise Competitive Binding**

Dana S. Marlin, Diego González Cabrera, David A. Leigh, and Alexandra M. Z. Slawin*

Although many carefully designed rotaxane-forming reactions have been developed in recent years,[1] new strategies[2] for switching the position of the macrocycle on the thread in response to an external trigger[3,4]—a key requirement for developing mechanical molecular devices based on such architectures[4]—remain rare. Competitive substrate binding is often used to bring about conformational changes that elicit function in biological "machines"[5] and has been successfully utilized in artificial host–guest systems,[6] chemical sensing,[7] and molecular Boolean logic operations.[8] However, as the macrocycle–thread interactions in a rotaxane are normally chosen so as to maximize the efficiency of the template mechanism, it is difficult to find competitive binders that can effectively disrupt these threaded and inherently self-organized complementary networks.[9,10] One elegant solution[11] to this problem is to utilize the preferred binding geometries of different metal d-orbital configurations (e.g. tetrahedral Cu^{I} →five-coordinate Cu^{II} or Zn^{II}) in transition-metal-based molecular shuttles.[12,13] Here we report an alternative solution, which does not involve a change in metal ion or oxidation state but uses the binding of a transition metal to move a macrocycle in a hydrogen-bonded molecular shuttle. Coordination of Cu^{II} or Cd^{II} ions to a bis(2-picolyl)amino (BPA)-derivatized glycine "station", followed by deprotonation of the adjacent amide group progressively wraps up the peptide station which leads to displacement of the macrocycle to an intrinsically weaker hydrogen-bonding site. In the case of Cu^{II}, the change in binding mode perturbs sensitive transitions within the d orbitals and the change in position of the shuttle is consequently accompanied by a color change.

The new shuttling strategy evolved out of the chance observation of an unusual controlled stepwise binding sequence of Cu^{II} ions to a multidentate ligand. Whilst attempting to develop methodology for the attachment of paramagnetic metal ions to macrocycles in rotaxanes, we prepared ligand H**1**,[14,15] which features a glycine residue substituted with two picoline units at its N terminus. Addition of $CuCl_2{\cdot}2H_2O$ to H**1** in CH_3CN led to the formation of H**1**$CuCl_2$, light blue crystals of which separated from the saturated liquors and gave the X-ray crystal structure shown in Figure 1a.[16] Cooling the solution of H**1**$CuCl_2$ to −20 °C in the presence of an additional half-equivalent of $CuCl_2{\cdot}2H_2O$ resulted in the deposition of large emerald-green crystals[17] of [H**1**$CuCl]_2[CuCl_4]$ on the walls of the flask which yielded the crystal structure shown in Figure 1b. Addition of one equivalent of NaH to solutions of either H**1**$CuCl_2$ or [H**1**-$(CuCl)]_2[CuCl_4]$ in *N*,*N*-dimethylformamide led to a third type of BPA–Cu^{II} complex as lime-green crystals of **1**CuCl (Figure 1c). The binding of the Cu^{II} ion—from the initial tridentate chelation of $CuCl_2$ to the BPA moiety in H**1**$CuCl_2$, to loss of a Cl^- ligand and coordination to the carbonyl oxygen of the amide group in $[H\mathbf{1}CuCl]^+$, and finally exchange of the carbonyl group for the nitrogen atom upon deprotonation of the amide group in **1**CuCl—results in progressive wrapping of the peptide unit around the metal (Figure 1).[18] We reasoned that integration of this stepwise changing coordination motif into a macrocycle-binding site in a peptide-based molecular shuttle might permit the complexation-controlled translocation of the macrocycle from one station to another.

To study the chemistry of the BPA-modified peptide station in a simple model system, we first prepared thread H_2**2**

[*] Dr. D. S. Marlin, D. González Cabrera, Prof. D. A. Leigh
School of Chemistry
University of Edinburgh
The King's Buildings
West Mains Road, Edinburgh EH93JJ (UK)
Fax: (+44) 131-667-9085
E-mail: david.leigh@ed.ac.uk
Prof. A. M. Z. Slawin
School of Chemistry
University of St. Andrews
Purdie Building, St. Andrews, Fife KY169ST (UK)

[**] This work was supported by the European Union Future and Emerging Technology Program Hy3M and the EPSRC. D.S.M. is a Marie Curie Fellow.

Supporting information for this article is available on the WWW under http://www.angewandte.org or from the author.

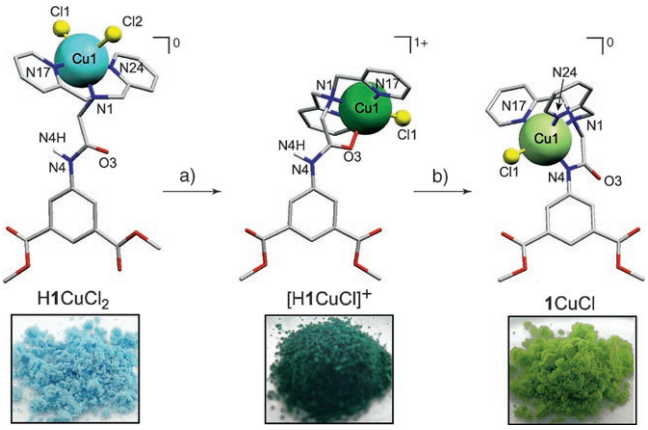

Figure 1. X-ray crystal structures[16] of H**1**$CuCl_2$ (initial), [H**1**CuCl]$^+$ (upon cooling[17]), and **1**CuCl (after addition of NaH) showing the change in binding mode of Cu^{II} to the multidentate ligand. C gray, Cl yellow, N blue, O red; all hydrogen atoms except the amide proton have been omitted for clarity. Reagents and conditions a) 0.5 equiv $CuCl_2 \cdot 2H_2O$, −20 °C, 100%; b) NaH or phosphazene P_1-*t*Bu base, 91%. The insets show photographs of the corresponding powdered, crystalline solids (from the left): H**1**$CuCl_2$, [H**1**CuCl]$_2$[$CuCl_4$], and **1**CuCl. Selected bond lengths [Å]: a) Cu1–N1 2.080, Cu1–N17 2.018, Cu1–N24 1.995, Cu1–Cl1 2.240, Cu1–Cl2 2.569; b) Cu1–N1 2.036, Cu1–N17 1.972, Cu1–N24 2.015, Cu1–Cl1 2.231, Cu1–O3 2.373; c) Cu1–N1 2.031, Cu1–N17 2.099, Cu1–N24 2.124, Cu1–Cl1 2.250, Cu1–N4 2.055.

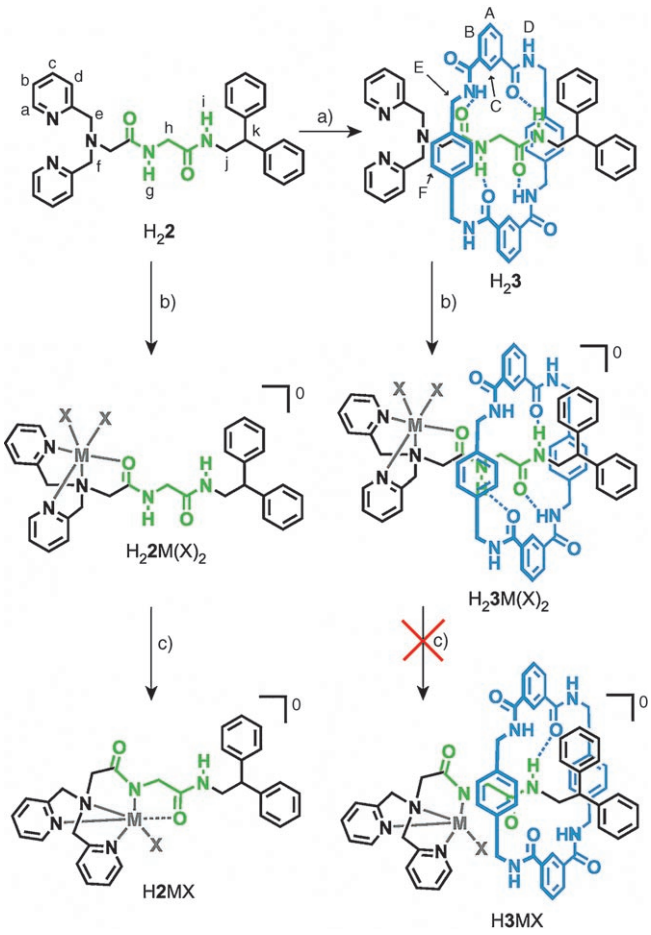

Scheme 1. Synthesis of [2]rotaxane H_2**3** from the BPA-glycylglycine thread H_2**2**, and their respective complexes with $CuCl_2$ and $Cd(NO_3)_2$ (≡MX_2). Reagents and conditions: a) *p*-xylylene diamine, isophthaloyl chloride, Et_3N, $CHCl_3$, 44%; b) $CuCl_2 \cdot 2H_2O$ or $Cd(NO_3)_2 \cdot 4H_2O$, 90% (H_2**2**$CuCl_2$), 90% (H_2**3**$CuCl_2$), 85% (H_2**2**$Cd(NO_3)_2$), 92% (H_2**3**$Cd(NO_3)_2$); c) NaH or phosphazene P_1-*t*Bu base, 77% (H**2**CuCl), 82% (H**2**$CdNO_3$). The coordination bond indicated by a dashed line in H**2**MX is only observed in the cadmium complex.

and rotaxane H_2**3** (Scheme 1). Formation of H_2**3** proceeded in 44% yield from H_2**2** (Scheme 1, a) which suggests that the affinity of the benzylic amide macrocycle for the BPA-glycylglycine station should be similar to that of other peptide-based stations, namely, intermediate between a strongly binding preorganized fumaramide group and a more weakly binding succinic amide ester moiety.[9a] The X-ray crystal structure of rotaxane H_2**3** shows that both carbonyl groups and both amide protons in the thread are involved in intercomponent hydrogen bonding to the macrocycle in the solid state (Figure 2b).[19]

The chelation geometries adopted by the BPA-glycylglycine station were studied by binding H_2**2** and H_2**3** to Cu^{II} as well as Cd^{II}, a diamagnetic metal that generally adopts ligand-coordination geometries that are similar to those of Cu^{II} with nitrogen-containing ligands, and attempted subsequent deprotonation of one of the amide groups (Scheme 1).[20] The X-ray crystal structures of several of the resulting complexes are shown in Figure 2, and the ^{1}H NMR spectra ([D_6]acetone,[21] 298 K) of the free ligands H_2**2** and H_2**3** and their complexes with $Cd(NO_3)_2$ are shown in Figure 3. The changes in the signals for the BPA protons (H_{a-f}) upon complexation of cadmium ions and the shielding of the protons of the peptide (H_h, H_j, and H_k) by the macrocycle in the rotaxanes compared to those of the thread confirm that the structures in solution are closely related to those in the solid state.

First, addition of $CuCl_2 \cdot 2H_2O$ or $Cd(NO_3)_2 \cdot 4H_2O$ to both the thread and rotaxane smoothly generated complexes of the type H_2**2**MX_2 and H_2**3**MX_2, respectively (M = Cu, Cd; Scheme 1, b). The solid-state structure of H_2**3**$Cd(NO_3)_2$ (Figure 2d) shows a coordination geometry which is similar to that of the intermediate [H**1**CuCl]$^+$ complex (Figure 1b), that is, featuring metal coordination to the carboxamide carbonyl oxygen.

Second, addition of one equivalent of a suitable base[22] (Scheme 1, c) to the thread intermediate complexes H_2**2**$CuCl_2$ and H_2**2**$Cd(NO_3)_2$ yielded H**2**CuCl and H**2**$CdNO_3$, respectively. The X-ray crystal structure of H**2**CuCl (Figure 2a) displays a Cu^{II} coordination sphere that is similar to that of **1**CuCl (Figure 1c) as well as an additional (albeit long at 3.188 Å) directional hydrogen bond between the proton (N7H) of the second amide group and the formal nitrogen anion (N4) of the coordinating carboxamido functionality. The X-ray crystal structure of H**2**$CdNO_3$ (Figure 2c) is closely related, but with the metal ion additionally coordinated to the carbonyl oxygen of the second carboxamide group. The binding of Cd^{II} (or Cu^{II}) ion to the BPA-glycine carbonyl oxygen presumably lowers the pK_a value of the adjacent NH proton in complexes of the type H_2**1**MX_2 and H_2**2**MX_2 which

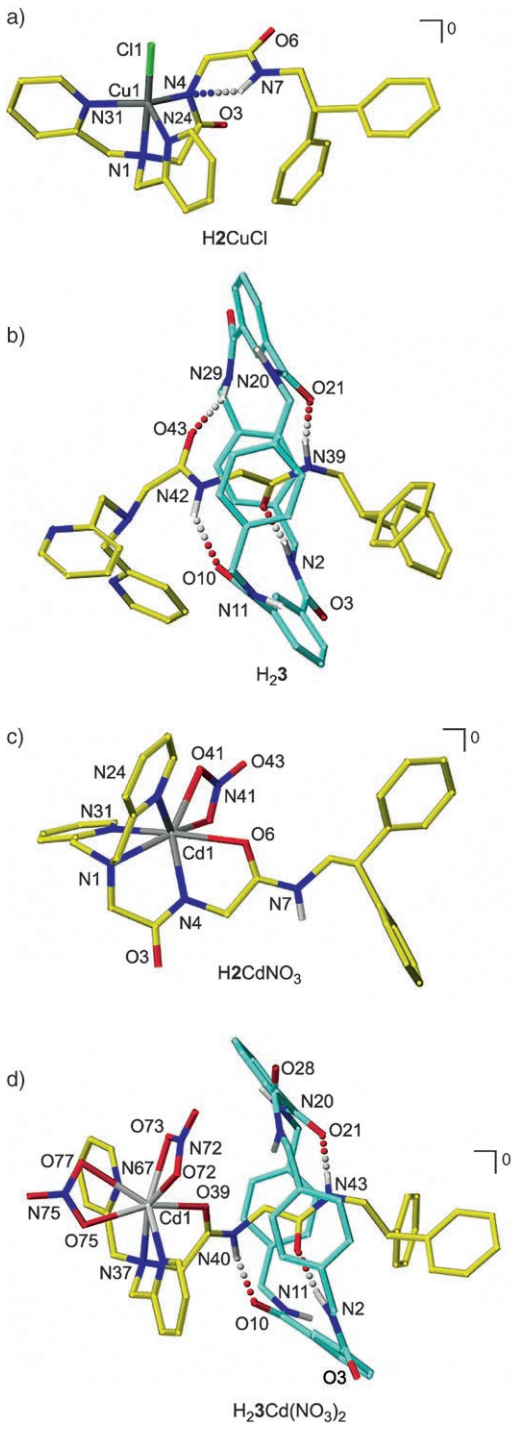

Figure 2. X-ray crystal structures[16] of a) H**2**CuCl, b) H_2**3**, c) H**2**$CdNO_3$, and d) H_2**3**$Cd(NO_3)_2$. C (thread) yellow, C (macrocycle) blue, metal atoms Cu^{II} and Cd^{II} gray; all hydrogen atoms except for the amide protons have been omitted for clarity. Selected bond lengths [Å]: a) Cu1–N1 2.052, Cu1–N4 1.968, Cu1–N24 2.176, Cu1–N31 2.079, Cu1–Cl1 2.238, N7H–N4 3.188; b) N2H–O40 1.877, N42H–O10 2.201, N39H–O21 1.944, N29H–O43 1.961; c) Cd1–N1 2.443, Cd1–N4 2.205, Cd1–O6 2.476, Cd1–N24 2.304, Cd1–N31 2.416, Cd1–O41 2.407, Cd1–O42 2.509; d) Cd1–N37 2.443, Cd1–N60 2.364, Cd1–N67 2.323, Cd1–O39 2.331, Cd1–O72 2.335, Cd1–O73 2.463, Cd1–O77 2.794, Cd1–O75 2.400, N43H–O21 1.863, N40H–O10 1.861, N2H–O42 2.017.

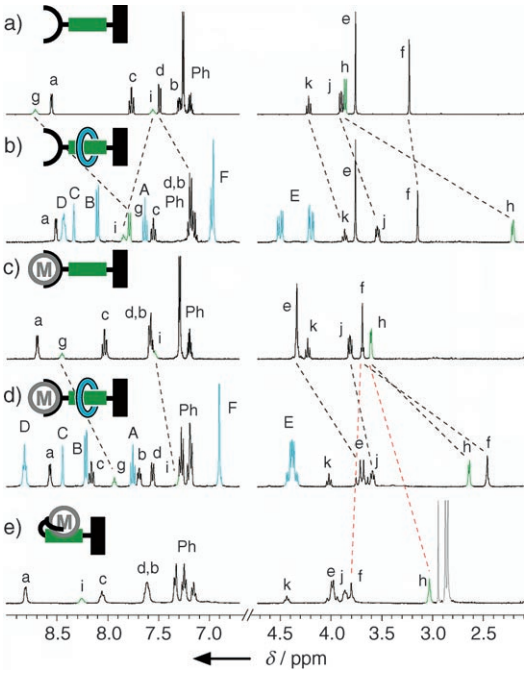

Figure 3. Partial ^{1}H NMR spectra (400 MHz, [D_6]acetone, 298 K) of a) H_2**2**, b) H_2**3**, c) H_2**2**$Cd(NO_3)_2$, d) H_2**3**$Cd(NO_3)_2$, and e) H**2**$CdNO_3$. Resonances colored and labeled as shown in Scheme 1. Peaks shown in light gray in part (e) originate from the phosphazene P_1-*t*Bu base.

allows *selective* deprotonation at this site.[23] However, neither of the metal coordination geometries shown in Figure 2 a or c would leave room on the peptide unit for a benzylic amide macrocycle to occupy, or sufficient hydrogen-bonding partners for it to bind to, in a rotaxane or molecular shuttle. Indeed, treatment of H_2**3**$CuCl_2$ or H_2**3**$Cd(NO_3)_2$ with strong bases[22] led to complicated reaction mixtures and significant degradation of the rotaxane structures, seemingly as a consequence of the macrocycle sterically preventing deprotonation of the coordination-activated carboxamide or adoption of the wrapped-up metal–ligand coordination architecture.

The model compounds confirm the generic basis of the stepwise binding chemistry and provide ^{1}H NMR spectroscopic fingerprints (Figure 3) of the various coordination modes, both with and without the macrocycle occupying the station. These spectra could be used to determine the position of the macrocycle in a more elaborate molecular shuttle, in particularly distinguishing between whether Cd^{II} is bound to a carbonyl oxygen or a carboxamido nitrogen atom and whether the macrocycle still occupies the BPA-glycylglycine station.

Accordingly, we prepared the two-station thread H_2**4** and rotaxane H_2**5** which feature BPA-derivatized glycylglycine (green) and succinic amide ester (orange) stations for the macrocycle (Scheme 2). The rationale behind the design was that although the ring would be expected to predominantly occupy the BPA-glycylglycine binding site in H_2**5**$Cd(NO_3)_2$, the ring would still spend some time away from the peptide station on the weaker binding succinic amide ester moiety. Whilst it is on the succinic amide ester station, the ring should

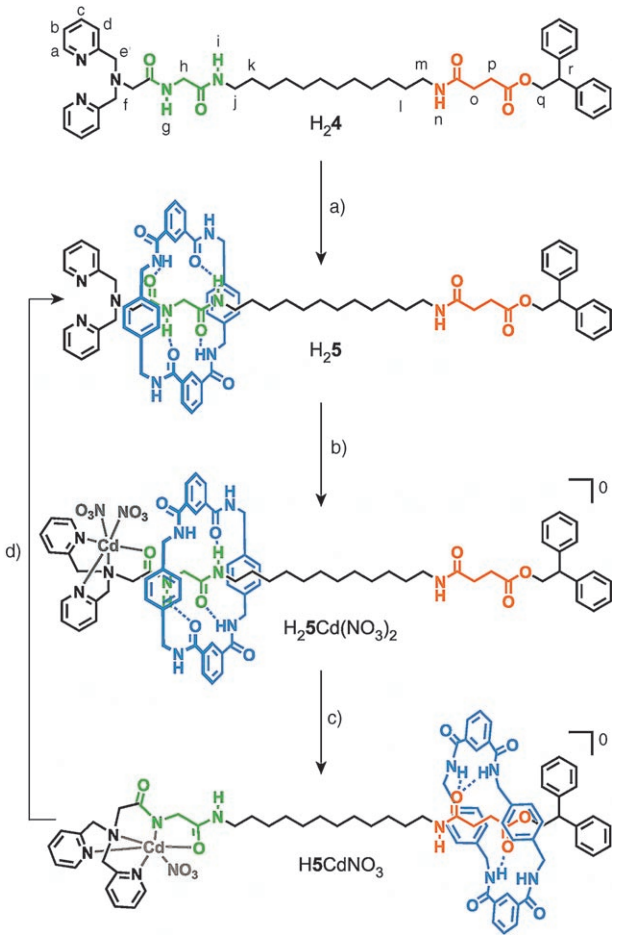

Scheme 2. Conversion of thread H_2**4** to rotaxane H_2**5**, and the reversible complexation of rotaxane H_2**5** with $Cd(NO_3)_2{\cdot}4H_2O$. Reagents and conditions: a) *p*-xylylene diamine, isophthaloyl chloride, Et_3N, $CHCl_3$, 22%; b) $Cd(NO_3)_2{\cdot}4H_2O$; c) phosphazene P_1-*t*Bu base; d) NaCN, NH_4Cl. Yields for conversions b–d were quantitative by ^{1}H NMR spectroscopic analysis.

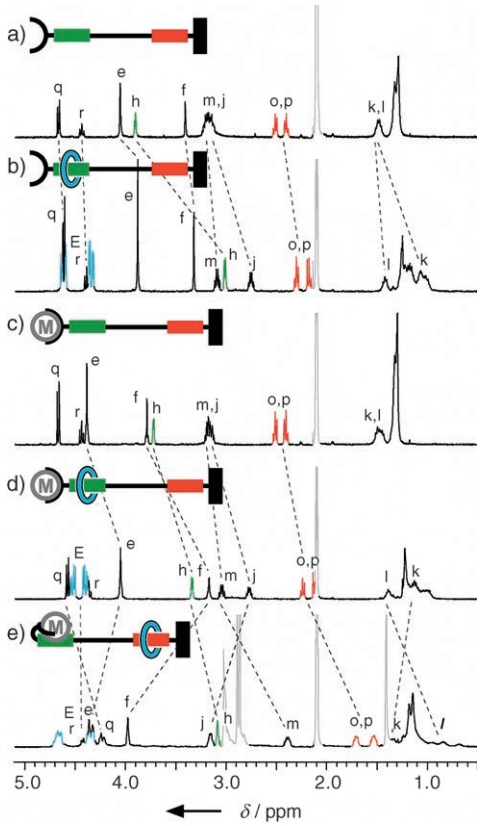

Figure 4. Partial ^{1}H NMR spectra (400 MHz, [D_6]acetone, 298 K) of a) H_2**4**, b) H_2**5**, c) H_2**4**$Cd(NO_3)_2$, d) H_2**5**$Cd(NO_3)_2$, and e) H**5**$CdNO_3$. Resonances colored and labeled as shown in Scheme 2. Peaks shown in light gray originate from residual nondeuterated solvent and, in part (e), the phosphazene P_1-*t*Bu base.

not sterically hinder the coordination-activated peptide (as it does so effectively in H_2**3**$Cd(NO_3)_2$, Scheme 1), so this minor translational isomer can then be selectively deprotonated at the carboxamide adjacent to the BPA unit. In accord with Le Chatelier's principle, H**5**$CdNO_3$ is formed. If the cadmium ion wraps itself up in the deprotonated glycylglycine residue in the manner seen with the model systems, this will switch off the peptide station and result in the macrocycle of H**5**$CdNO_3$ predominately occupying the succinic amide ester station (Scheme 2).

Pleasingly, the ^{1}H NMR spectra of the rotaxanes and threads (shown in Figure 4) were fully consistent with the predicted behavior. The relative shielding of the peptide protons in the ^{1}H NMR spectrum of H_2**5** compared to H_2**4** (Figure 4a and b, respectively) confirms that the occupancy of the macrocycle is approximately 90:10 in favor of the glycylglycine station in [D_6]acetone at 298 K.[21] Addition of one equivalent of $Cd(NO_3)_2{\cdot}4H_2O$ to H_2**4** and H_2**5** to form H_2**4**$Cd(NO_3)_2$ and H_2**5**$Cd(NO_3)_2$, respectively (Scheme 2, b), resulted in little change (except for the BPA protons) in the ^{1}H NMR spectra in [D_6]acetone at room temperature (compare Figures 4c and d with Figures 4a and b, respectively), indicating that the preferred position of the macrocycle remains unchanged despite chelation of the terminal peptide carbonyl group to a metal — the shifts experienced by the protons around the metal-binding region, for example, H_f and H_h, are similar to those in H_2**3**$Cd(NO_3)_2$ (Figure 3d). However, subsequent deprotonation of the amide proton H_g of H_2**5**$Cd(NO_3)_2$ with one equivalent of phosphazene base P_1-*t*Bu[22] (Scheme 2, c) causes major changes (Figure 4e). The upfield shifts of H_m, H_o, and H_p ($\delta = 3.2$, 2.5, and 2.4 ppm in H_2**4**$Cd(NO_3)_2$ (Figure 4c) to $\delta = 2.4$, 1.7, and 1.5 ppm, respectively) are clear evidence for the translocation of the macrocycle to the succinic amide ester station (marked in orange). Similarly, the downfield shift of H_f ($\delta = 3.2$ ppm in H_2**5**$Cd(NO_3)_2$ (Figure 4d) to $\delta = 4.0$ ppm) and the restoration of H_j to its position at $\delta = 3.2$ ppm in the thread (Figure 4c) show that the peptide station (marked in green) is no longer occupied by the benzylic amide macrocycle. The small upfield movement in H_h is consistent with the shift brought about by coordination of the deprotonated amide group to the metal, as seen with H**2**$CdNO_3$ (Figure 3e).

The transition-metal-binding-induced translocation of the macrocycle in the hydrogen-bonded shuttle is fully reversible (Scheme 2, d). Removal of the Cd^{II} ion from H**5**$CdNO_3$ with

excess CN^- and reprotonation of the amide nitrogen atom with NH_4Cl quantitatively regenerates H_2**5**.

Finally, indirect evidence for a similar shuttling mechanism using Cu^{II} binding is provided by the change in absorption of weak (likely d–d) transitions in the low-energy region of the UV/Vis spectrum of H_2**5**$CuCl_2$ upon addition of P_1-*t*Bu (Figure 5). The color change that occurs

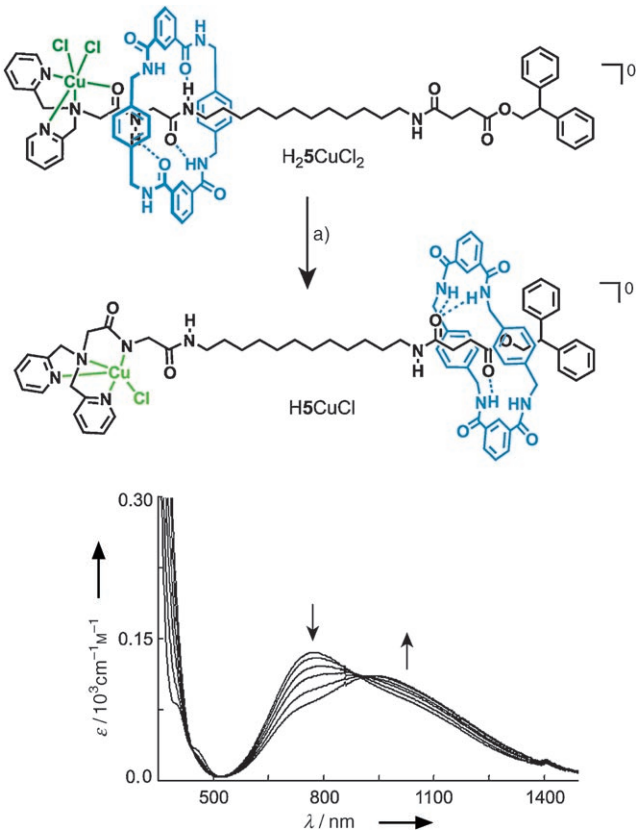

Figure 5. Change in absorption spectrum for H_2**5**$CuCl_2$ upon addition of a) phosphazene P_1-*t*Bu base (up to 1 equivalent).

during a single-spot-to-single-spot transformation, as revealed by thin layer chromatographic analysis, is almost indistinguishable to that observed during the conversion of [H**1**CuCl]$^+$ to **1**CuCl (Figure 1). As the base-promoted transformation (H_2**3**$CuCl_2$→H**3**CuCl) does *not* occur for the short rotaxane (Scheme 1, c), yet *does* take place for H_2**5**$CuCl_2$→H**5**CuCl (Figure 5), it seems reasonable to conclude that the color change is accompanied by the same change in the position of macrocycle that occurs in the cadmium-coordinated molecular shuttle (Scheme 2, c).

In conclusion, we have described a mechanism through which a large amplitude mechanical movement can be induced within a hydrogen-bonded molecular shuttle by the stepwise competitive binding of transition-metal ions. The peptide station is progressively wrapped up by the metal which disrupts hydrogen-bonding interactions between the station and macrocycle and causes displacement of the macrocycle to a second station. The control over shuttling while the metal is bound to the thread provides two well-defined states in which the macrocycle is held either close to or distant from a single metal atom. This feature could be used to construct rotaxanes that display the intriguing property of being able to switch the distance between two metal centers, which are not connected by chemical bonds, by an externally triggered mechanical motion.

Received: May 21, 2005
Revised: June 21, 2005
Published online: November 28, 2005

Keywords: coordination modes · molecular devices · noncovalent interactions · rotaxanes · transition metals

[1] For some recent examples of new rotaxane syntheses, see: a) K. M. Wollyung, K. T. Xu, M. Cochran, A. M. Kasko, W. L. Mattice, C. Wesdemiotis, C. Pugh, *Macromolecules* **2005**, *38*, 2574–2586; b) N. Kihara, S. Motoda, T. Yokozawa, T. Takata, *Org. Lett.* **2005**, *7*, 1199–1202; c) H. P. Kwan, T. M. Swager, *J. Am. Chem. Soc.* **2005**, *127*, 5902–5909; d) M. Miyauchi, T. Hoshino, H. Yamaguchi, S. Kamitori, A. Harada, *J. Am. Chem. Soc.* **2005**, *127*, 2034–2035; e) B. A. Blight, K. A. Van Noortwyk, J. A. Wisner, M. C. Jennings, *Angew. Chem.* **2005**, *117*, 1523–1528; *Angew. Chem. Int. Ed.* **2005**, *44*, 1499–1504; f) D. J. Hoffart, S. J. Loeb, *Angew. Chem.* **2005**, *117*, 923–926; *Angew. Chem. Int. Ed.* **2005**, *44*, 901–904; g) I. Yoon, M. Narita, T. Shimizu, M. Asakawa, *J. Am. Chem. Soc.* **2004**, *126*, 16740–16741; h) Y. Furusho, T. Matsuyama, T. Takata, T. Moriuchi, T. Hirao, *Tetrahedron Lett.* **2004**, *45*, 9593–9697; i) N. Kihara, M. Hashimoto, T. Takata, *Org. Lett.* **2004**, *6*, 1693–1696; j) M. J. Gunter, S. M. Farquhar, K. M. Mullen, *New J. Chem.* **2004**, *28*, 1443–1449; k) W. C. Hung, K. S. Liao, Y. H. Liu, S. M. Peng, S. H. Chiu, *Org. Lett.* **2004**, *6*, 4183–4186; l) K. Hiratani, M. Kaneyama, Y. Nagawa, E. Koyama, M. Kanesato, *J. Am. Chem. Soc.* **2004**, *126*, 13568–13569; m) K. J. Chang, Y. J. An, H. Uh, K. S. Jeong, *J. Org. Chem.* **2004**, *69*, 6556–6563; n) W. Abraham, L. Grubert, U. W. Grummt, K. Buck, *Chem. Eur. J.* **2004**, *10*, 3562–3568; o) H. Georges, S. J. Loeb, J. Tiburcio, J. A. Wisner, *Org. Biomol. Chem.* **2004**, *2*, 2751–2756; p) A. Orita, J. Okano, Y. Tawa, L. S. Jiang, J. Otera, *Angew. Chem.* **2004**, *116*, 3810–3814; *Angew. Chem. Int. Ed.* **2004**, *43*, 3724–3728; q) P. Ballester, M. Capo, A. Costa, P. M. Deya, A. Frontera, R. Gomila, *Molecules* **2004**, *9*, 278–286; r) Y. Furusho, T. Oku, G. A. Rajkumar, T. Takata, *Chem. Lett.* **2004**, *33*, 52–53; s) D. Tuncel, J. H. G. Steinke, *Macromolecules* **2004**, *37*, 288–302; t) J. Terao, A. Tang, J. J. Michels, A. Krivokapic, H. L. Anderson, *Chem. Commun.* **2004**, 56–57; u) J. D. Badjic, V. Balzani, A. Credi, S. Silvi, J. F. Stoddart, *Science* **2004**, *303*, 1845–1849; v) J. S. Hannam, S. M. Lacy, D. A. Leigh, C. G. Saiz, A. M. Z. Slawin, S. G. Stitchell, *Angew. Chem.* **2004**, *116*, 3322–3326; *Angew. Chem. Int. Ed.* **2004**, *43*, 3260–3264.

[2] a) D. A. Leigh, E. M. Pérez, *Chem. Commun.* **2004**, 2262–2263; b) B. W. Laursen, S. Nygaard, J. O. Jeppesen, J. F. Stoddart, *Org. Lett.* **2004**, *6*, 4167–4170.

[3] R. A. Bissell, E. Córdova, A. E. Kaifer, J. F. Stoddart, *Nature* **1994**, *369*, 133–137.

[4] a) *Molecular Catenanes, Rotaxanes, and Knots: A Journey Through the World of Molecular Topology* (Eds.: J.-P. Sauvage, C. Dietrich-Buchecker), Wiley-VCH, Weinheim, **1999**; b) V. Balzani, A. Credi, F. M. Raymo, J. F. Stoddart, *Angew. Chem.* **2000**, *112*, 3484–3530; *Angew. Chem. Int. Ed.* **2000**, *39*, 3348–3391; c) V. Balzani, M. Venturi, A. Credi, *Molecular Devices and*

Machines—A Journey into the Nanoworld, Wiley-VCH, Weinheim, **2003**; d) A. H. Flood, R. J. A. Ramirez, W.-Q. Deng, R. P. Muller, W. A. Goddard, J. F. Stoddart, *Aust. J. Chem.* **2004**, *57*, 301 – 322; e) "Synthetic Molecular Machines": E. R. Kay, D. A. Leigh, *Functional Artificial Receptors* (Eds.: T. Schrader, A. D. Hamilton), Wiley-VCH, Weinheim, **2005**, pp. 333 – 406.

[5] For example, see: A. Saghatelian, K. M. Guckian, D. A. Thayer, M. R. Ghadiri, *J. Am. Chem. Soc.* **2003**, *125*, 344 – 345.

[6] For example, see: a) A. Credi, M. Montalti, V. Balzani, S. J. Langford, F. M. Raymo, J. F. Stoddart, *New J. Chem.* **1998**, *22*, 1061 – 1065; b) M. Asakawa, S. Iqbal, J. F. Stoddart, N. D. Tinker, *Angew. Chem.* **1996**, *108*, 1054 – 1056; *Angew. Chem. Int. Ed. Engl.* **1996**, *35*, 976 – 978.

[7] For example, see: L. A. Cabell, E. V. Anslyn, *Tetrahedron Lett.* **1999**, *40*, 7753 – 7756.

[8] For example, see: R. Ballardini, V. Balzani, A. Credi, M. T. Gandolfi, S. J. Langford, S. Menzer, L. Prodi, J. F. Stoddart, M. Venturi, D. J. Williams, *Angew. Chem.* **1996**, *108*, 1056 – 1059; *Angew. Chem. Int. Ed. Engl.* **1996**, *35*, 978 – 981.

[9] Intercomponent noncovalent interactions are inherently strengthened by preorganization within a rotaxane architecture (see: D. A. Leigh, P. J. Lusby, A. M. Z Slawin, D. B. Walker, *Angew. Chem.* **2005**, *117*, 4633 – 4640; *Angew. Chem. Int. Ed.* **2005**, *44*, 4557 – 4564). For example, the benzylic amide macrocycle in fumaramide-based molecular shuttles remains held in place[9a] by four macrocycle–thread amide–amide hydrogen bonds ($\beta_{amide} = 8.3$[9b]) even in neat [D$_6$]DMSO ($\beta_{DMSO} = 8.9$[9b]). a) A. Altieri, G. Bottari, F. Dehez, D. A. Leigh, J. K. Y. Wong, F. Zerbetto, *Angew. Chem.* **2003**, *115*, 2398 – 2402; *Angew. Chem. Int. Ed.* **2003**, *42*, 2296 – 2300; b) C. A. Hunter, *Angew. Chem.* **2004**, *116*, 5424 – 5439; *Angew. Chem. Int. Ed.* **2004**, *43*, 5310 – 5324.

[10] S. A. Vignon, T. Jarrosson, T. Iijima, H.-R. Tseng, J. K. M. Sanders, J. F. Stoddart, *J. Am. Chem. Soc.* **2004**, *126*, 9884 – 9885.

[11] a) D. J. Cárdenas, A. Livoreil, J.-P. Sauvage, *J. Am. Chem. Soc.* **1996**, *118*, 11980 – 11981; b) A. Livoreil, J.-P. Sauvage, N. Armaroli, V. Balzani, L. Flamigni, B. Ventura, *J. Am. Chem. Soc.* **1997**, *119*, 12114 – 12124; c) J.-P. Collin, P. Gaviña, J.-P. Sauvage, *New J. Chem.* **1997**, *21*, 525 – 528; d) N. Armaroli, V. Balzani, J.-P. Collin, P. Gaviña, J.-P. Sauvage, B. Ventura, *J. Am. Chem. Soc.* **1999**, *121*, 4397 – 4408; e) L. Raehm, J.-M. Kern, J.-P. Sauvage, *Chem. Eur. J.* **1999**, *5*, 3310 – 3317; f) M. C. Jiménez, C. Dietrich-Buchecker, J.-P. Sauvage, *Angew. Chem.* **2000**, *112*, 3422 – 3425; *Angew. Chem. Int. Ed.* **2000**, *39*, 3284 – 3287; g) M. C. Jiménez-Molero, C. Dietrich-Buchecker, J.-P. Sauvage, *Chem. Eur. J.* **2002**, *8*, 1456 – 1466; h) M. C. Jiménez-Molero, C. Dietrich-Buchecker, J.-P. Sauvage, *Chem. Commun.* **2003**, 1613 – 1616; i) I. Poleschak, J. -M, Kern, J.-P. Sauvage, *Chem. Commun.* **2004**, 474 – 476; j) P. Mobian, J.-M. Kern, J.-P. Sauvage, *Angew. Chem.* **2004**, *116*, 2446 – 2449; *Angew. Chem. Int. Ed.* **2004**, *43*, 2392 – 2395; k) J.-P. Sauvage, *Chem. Commun.* **2005**, 1507 – 1510.

[12] For recent reviews on the synthesis of interlocked molecules using transition-metal templates, see: a) T. J. Hubin, D. H. Busch, *Coord. Chem. Rev.* **2000**, *200–202*, 5 – 52; b) J.-P. Collin, C. Dietrich-Buchecker, P. Gaviña, M. C. Jiménez-Molero, J.-P. Sauvage, *Acc. Chem. Res.* **2001**, *34*, 477 – 487; c) M. J. Blanco, J. C. Chambron, M. C. Jiménez, J.-P. Sauvage, *Top. Stereochem.* **2003**, *23*, 125 – 173; d) S. J. Cantrill, K. S. Chichak, A. J. Peters, J. F. Stoddart, *Acc. Chem. Res.* **2005**, *38*, 1 – 9; see also: e) A. C. Try, M. M. Harding, D. G. Hamilton, J. K. M. Sanders, *Chem. Commun.* **1998**, 723 – 724; f) M. E. Padilla-Tosta, O. D. Fox, M. G. B. Drew, P. D. Beer, *Angew. Chem.* **2001**, *113*, 4365 – 4369; *Angew. Chem. Int. Ed.* **2001**, *40*, 4235 – 4239; g) D. A. Leigh, P. J. Lusby, S. J. Teat, A. J. Wilson, J. K. Y. Wong, *Angew. Chem.* **2001**, *113*, 1586 – 1591; *Angew. Chem. Int. Ed.* **2001**, *40*, 1538 – 1543; h) C. P. McArdle, S. Van, M. C. Jennings, R. J. Puddephatt, *J. Am. Chem. Soc.* **2002**, *124*, 3959 – 3965; i) L. Hogg, D. A. Leigh, P. J. Lusby, A. Morelli, S. Parsons, J. K. Y. Wong, *Angew. Chem.* **2004**, *116*, 1238 – 1241; *Angew. Chem. Int. Ed.* **2004**, *43*, 1218 – 1221; j) W. W. H. Wong, J. Cookson, E. A. L. Evans, E. J. L. McInnes, J. Wolowska, J. P. Maher, P. Bishop, P. D. Beer, *Chem. Commun.* **2005**, 2214 – 2216.

[13] For reviews on the synthesis of interlocked structures using transition-metal connectors, see: a) M. Fujita, *Acc. Chem. Res.* **1999**, *32*, 53 – 61; b) K. Kim, *Chem. Soc. Rev.* **2002**, *31*, 96 – 107; c) S. R. Batten, R. Robson, *Angew. Chem.* **1998**, *110*, 1558 – 1595; *Angew. Chem. Int. Ed.* **1998**, *37*, 1460 – 1494; d) A. J. Blake, N. R. Champness, P. Hubberstey, W.-S. Li, M. A. Withersby, M. Schröder, *Coord. Chem. Rev.* **1999**, *183*, 117 – 138; e) S. J. Loeb, *Chem. Commun.* **2005**, 1511 – 1518.

[14] a) D. D. Cox, S. J. Benkovic, L. M. Bloom, F. C. Bradley, M. J. Nelson, L. Que, Jr., D. E. Wallick, *J. Am. Chem. Soc.* **1988**, *110*, 2026 – 2032; Complexes of this type of ligand have previously only been reported in a single tetradentate form; see: b) S. Ito, T. Okuno, H. Matsushima, T. Tokli, Y. Nishida, *J. Chem. Soc. Dalton Trans.* **1996**, 4479 – 4484; c) T. Okuno, S. Ohba, Y. Nishida, *Polyhedron* **1997**, *16*, 3765 – 3774; d) T. Kobayashi, T. Okuno, M. Kunita, S. Ohba, Y. Nishida, *Polyhedron* **1998**, *17*, 1553 – 1559; e) N. Niklas, O. Walter, R. Alsfasser, *Eur. J. Inorg. Chem.* **2000**, 1723 – 1731; f) N. Niklas, S. Wolf, G. Liehr, C. E. Anson, A. K. Powell, R. Alsfasser, *Inorg. Chim. Acta* **2001**, *314*, 126 – 132; g) C. Incarvito, A. L. Rheingold, A. L. Gavrilova, C. Jin Qin, B. Bosnich, *Inorg. Chem.* **2001**, *40*, 4101 – 4108; h) N. Niklas, F. Hampel, O. Walter, G. Liehr, R. Alsfasser, *Eur. J. Inorg. Chem.* **2002**, 1839 – 1847; i) A. L. Gavrilova, C. Jin Qin, R. D. Sommer, A. L. Rheingold, B. Bosnich, *J. Am. Chem. Soc.* **2002**, *124*, 1714 – 1722; j) N. Niklas, O. Walter, F. Hampel, R. Alsfasser, *J. Chem. Soc. Dalton Trans.* **2002**, 3367 – 3373.

[15] H**1** = 5-[2-(bis(pyridin-2-ylmethyl)amino)acetyl)amino]isophthalic acid dimethyl ester; H$_2$**2** = 2-(bis(pyridin-2-ylmethyl)amino)-*N*-[(2,2-diphenyl-ethylcarbamoyl)methyl]acetamide; H$_2$**3** = ([2](1,7,14,20-tetraaza-2,6,15,19-tetraoxo-3,5,9,12,16,18,22,25-tetrabenzocyclohexacosane)-(2-(bis(pyridin-2-ylmethyl)amino)-*N*-[(2,2-diphenylethylcarbamoyl)methyl]acetamide) rotaxane; H$_2$**4** = 2,2-diphenylethyl 4-(12-(2-(2-(bis(pyridine-2-ylmethyl)amino)acetamido)acetamido)dodecylamino-4-oxobutanoate; H$_2$**5** = ([2](1,7,14,20-tetraaza-2,6,15,19-tetraoxo-3,5,9,12,16,18,22,25-tetrabenzocyclohexacosane)-(2,2-diphenylethyl 4-(12-(2-(2-(bis(pyridine-2-ylmethyl)amino)acetamido)acetamido)dodecylamino-4-oxobutanoate) rotaxane.

[16] X-ray crystal structural data for H**1**CuCl$_2$, [H**1**CuCl]$_2$[CuCl$_4$], H$_2$**3**, H**2**CdNO$_3$, and H$_2$**3**Cd(NO$_3$)$_2$ were collected at 93 K using a Rigaku Saturn (MM007 high-flux RA/Mo$_{K\alpha}$ radiation, confocal optic), while those for **1**CuCl and H**2**CuCl were collected at 93 K using a Mercury (MM007 high-flux RA/Mo$_{K\alpha}$ radiation, confocal optic). All data collections employed narrow frames (0.3–1.0°) to obtain at least a full hemisphere of data. Intensities were corrected for Lorentz polarization and absorption effects (multiple equivalent reflections). Structures were solved by direct methods, non-hydrogen atoms were refined anisotropically, with C–H protons refined in riding geometries (SHELXTL) against F^2. In most cases, amide protons were refined isotropically subject to a distant constraint. The protons on solvate molecules were not allowed for in the refinement. Data for H**1**CuCl$_2$·0.5 CH$_3$CN·0.055 H$_2$O: $C_{25}H_{25.61}Cl_2CuN_{4.5}O_{5.06}$, $M = 604.44$, crystal size $0.1 \times 0.05 \times 0.01$ mm^3, trigonal, $P\bar{3}$, $a = 40.804(2)$, $c = 8.4772(4)$ Å, $Z = 18$, $\rho_{calcd} = 1.478$ Mg m^{-3}; $\mu = 1.044$ mm^{-1}, 91570 collected, 14360 unique ($R_{int} = 0.0825$), $R = 0.1258$ for 12778 observed data [$F_o > 4\sigma(Fo)$], $S = 1.189$ for 1037 parameters. Residual electron density extremes were 1.500 and -1.250 e Å^{-3}. Data for [H**1**CuCl]$_2$[CuCl$_4$]·0.5 H$_2$O: $C_{48}H_{49}Cl_6Cu_3N_8O_{10.5}$, $M = 1309.27$, crystal size $0.1 \times 0.05 \times 0.03$ mm^3, monoclinic, $P2(1)/n$, $a = 8.1667(16)$, $b = 30.257(5)$, $c = 23.377(4)$ Å, $Z = 4$, $\rho_{calcd} = 1.506$ Mg m^{-3}; $\mu = 1.433$ mm^{-1},

51258 collected, 11852 unique ($R_{int}=0.0484$), $R=0.1234$ for 9492 observed data [$F_o>4\sigma(F_o)$], $S=1.540$ for 691 parameters. Residual electron density extremes were 2.381 and −1.117 e Å^{-3}. Data for **1**CuCl: $C_{24}H_{23}ClCuN_4O_5$, $M=546.45$, crystal size 0.2 × 0.1 × 0.1 mm^3, monoclinic, $C2/c$, $a=14.026(3)$, $b=11.390(3)$, $c=30.259(6)$ Å, $Z=8$, $\rho_{calcd}=1.513$ Mg m^{-3}; $\mu=1.065$ mm^{-1}, 9975 collected, 3728 unique ($R_{int}=0.0644$), $R=0.0456$ for 3104 observed data [$F_o>4\sigma(F_o)$], $S=1.024$ for 329 parameters. Residual electron density extremes were 0.472 and −0.383 e Å^{-3}. Data for H**2**CuCl: $C_{30}H_{30}ClCuN_5O_2$, $M=591.58$, crystal size 0.2 × 0.1 × 0.1 mm^3, monoclinic, $P2(1)/n$, $a=16.089(3)$, $b=9.9833(18)$, $c=16.968(3)$ Å, $Z=4$, $\rho_{calcd}=1.446$ Mg m^{-3}; $\mu=0.940$ mm^{-1}, 15979 collected, 4822 unique ($R_{int}=0.0333$), $R=0.0486$ for 4460 observed data [$F_o>4\sigma(F_o)$], $S=1.053$ for 357 parameters. Residual electron density extremes were 2.384 and −0.553 e Å^{-3}. Data for H_2**3**: $C_{68}H_{71}N_9O_8$, $M=1142.34$, crystal size 0.2 × 0.1 × 0.05 mm^3, monoclinic, $P2(1)/c$, $a=13.0505(10)$, $b=19.1256(14)$, $c=25.970(2)$ Å, $Z=4$, $\rho_{calcd}=1.183$ Mg m^{-3}; $\mu=0.079$ mm^{-1}, 45077 collected, 11321 unique ($R_{int}=0.1105$), $R=0.1789$ for 10284 observed data [$F_o>4\sigma(F_o)$], $S=1.190$ for 793 parameters. Residual electron density extremes were 1.387 and −0.435 e Å^{-3}. Data for H**2**$CdNO_3$: $C_{30}H_{30}CdN_6O_5$, $M=667.00$, crystal size 0.15 × 0.15 × 0.05 mm^3, monoclinic, $P2(1)/c$, $a=9.8549(14)$, $b=17.620(3)$, $c=16.444(3)$ Å, $Z=4$, $\rho_{calcd}=1.553$ Mg m^{-3}; $\mu=0.817$ mm^{-1}, 20308 collected, 4953 unique ($R_{int}=0.0301$), $R=0.0285$ for 4357 observed data [$F_o>4\sigma(F_o)$], $S=1.085$ for 384 parameters. Residual electron density extremes were 0.872 and −0.334 e Å^{-3}. Data for H_2**3**$Cd(NO_3)_2$: $C_{62}H_{59}CdN_{11}O_{12}$, $M=1262.6$, crystal size 0.1 × 0.1 × 0.03 mm^3, monoclinic, $C2/c$, $a=28.252(13)$, $b=10.588(5)$, $c=42.457(19)$ Å, $Z=8$, $\rho_{calcd}=1.439$ Mg m^{-3}; $\mu=0.426$ mm^{-1}, 27366 collected, 9652 unique ($R_{int}=0.0925$), $R=0.0814$ for 5850 observed data [$F_o>4\sigma(F_o)$], $S=1.076$ for 857 parameters. Residual electron density extremes were 0.976 and −0.640 e Å^{-3}. CCDC 269894–269900 contain the supplementary crystallographic data for this paper. These data can be obtained free of charge from The Cambridge Crystallographic Data Centre via www.ccdc.cam.ac.uk/data_request/cif.

[17] Some of the emerald-green color of [H**1**CuCl]$_2$[$CuCl_4$] can be attributed to the [$CuCl_4$]$^{2-}$ counterion.

[18] Wrapped up metal–peptide complexes are widely seen in biological contexts, for example, with copper and various tripeptide ligands; see: a) H. Sigel, R. B. Martin, *Chem. Rev.* **1982**, *82*, 385 – 426; b) P. Deschamps, P. P. Kulkarni, M. Gautam-Basak, B. Sarkar, *Coord. Chem. Rev.* **2005**, *249*, 895 – 909. However, the use of a designed auxiliary ligand attached to the peptide that facilitates stepwise control over the binding modes is, to the best of our knowledge, unknown.

[19] Several different hydrogen-bonding motifs are in equilibrium in solution. G. W. H. Wurpel, A. M. Brouwer, I. H. M. van Stokkum, A. Farran, D. A. Leigh, *J. Am. Chem. Soc.* **2001**, *123*, 11327 – 11328.

[20] Cd^{II} exhibits a strong binding affinity and kinetic stability for BPA-type ligands [for example, see: N. Niklas, F. Hampel, G. Liehr, A. Zahl, R. Alsfasser, *Chem. Eur. J.* **2001**, *7*, 5135 – 5141], and its stable diamagnetic ground state allows the characterization of complexes by ^{1}H NMR spectroscopy.

[21] The molecular shuttle rotaxane and thread cadmium complexes were insufficiently soluble in $CDCl_3$ or CD_2Cl_2 for ^{1}H NMR spectroscopic studies so [D_6]acetone was used throughout.

[22] For the metal complexes of the short thread, H_2**2**, either NaH or Schwesinger's phosphazene P_1-*t*Bu base (*N*′-*tert*-butyl-*N*,*N*,*N*′,*N*′,*N*″,*N*″-hexamethylphosphorimidic triamide) [R. Schwesinger, C. Hasenfratz, H. Schlemper, L. Walz, E.-M. Peters, K. Peters, H. G. von Schnering, *Angew. Chem.* **1993**, *105*, 1420 – 1422; *Angew. Chem. Int. Ed. Engl.* **1993**, *32*, 1361 – 1363] could be used to deprotonate BPA at its terminal amide group. However, for H_2**4** and H_2**5**, which contain an ester linkage, only P_1-*t*Bu proved suitable.

[23] Without this discrimination, the more-complicated molecular shuttle system containing multiple amide groups would not be able to function.

